Swarm and Evolutionary Computation 65 (2021) 100926

Contents lists available at ScienceDirect

Swarm and Evolutionary Computation

journal homepage: www.elsevier.com/locate/swevo

Stable switched controllers for a swarm of UGVs for hierarchal landmark navigation

Sandeep A. Kumar, B. Sharma*, J. Vanualailai, A. Prasad

School of Information Technology, Engineering, Mathematics & Physics, The University of the South Pacific, Fiji

ARTICLE INFO

2010 MSC:
00-01
99-00

Keywords:
Lagrangian swarm
Switched system
Multiple lyapunov functions
Switching signal
Velocity controllers

ABSTRACT

This paper presents the development of a new set of switched velocity controllers of a swarm of unmanned ground vehicles (UGVs) from multiple Lyapunov functions, which are invoked according to a switching rule. The Lyapunov-based Control Scheme (LbCS) has derived the multiple Lyapunov functions that fall under the artificial potential field method of the classical approach. Interaction of the three main pillars of LbCS, which are safety, shortness, and smoothest path for motion planning, bring about cost and time effectiveness and efficiency of the velocity controllers. The switched controllers enable the UGVs to navigate autonomously via hierarchal landmarks in a cluttered workspace to their equilibrium state. The switched controllers give rise to a switched system whose stability is proven using Branicky's stability criteria for switched systems based on multiple Lyapunov functions. Simulations results are presented to show the effectiveness of the nonlinear time-invariant controllers. Later, effects of noise are included in the velocity controllers to show system robustness.

1. Introduction

The recent past decades have seen unprecedented attention, importance, and investment given to robots by researchers, academics, sponsors, and industries, with an exponential growth in real-world applications related especially to human livelihood and endeavors, and found in most sectors that have complicated, dull, dangerous, and dirty environments[1,2], and mostly requiring automation, repetition, and high work rates [3,4]. These real-life applications include surveillance, transportation, save and rescue, pursuit-evasion, pedestrian navigation, waste management, foraging, entertainment, and media, pick and place, surveying, and explorations [1,2,5–8]. An extensive array of robotic systems such as mobile manipulators, anchored and unanchored arms, car-like, tractor-trailer, aerial and underwater robots, swimming and flying robots, and parallel robots have been designed to operationalize these real-life applications [9–14]. Additionally, we now have a strong presence of assistive robots such as robotics pets, surgical robots, telesurgery robots, and companionship robots in the health and social care for surgery, company, monitoring, elderly assistance, and handicap assistance, to name a few major ones [15].

The emergence of swarm robotics is commendable in providing solutions to problems where general robotics would turn out to be less efficient in terms of sensing capabilities, situation awareness, robustness to a mission failure, sharing of workload, search and rescue. Swarm robotics is an approach to the coordination of multiple robots as a system that consists of large numbers of mostly simple physical robots [16]. Swarm intelligence is nature-inspired but is not limited by the emergent behaviour observed in social insects. The attempts of researchers to comprehend biological swarming can be categorized into two different modeling approaches: the *Eulerian* and the *Lagrangian* approaches [5,17–21]. In the Eulerian approach, the swarm is considered a *continuum* described by its density in one-, two- or three-dimensional space. Partial differential equations describe the time evolution of swarm density. In the Lagrangian approach, the state (position, instantaneous velocity or instantaneous acceleration) of each individual and its relationship with other individuals in the swarm is studied; it is an *individual-based* approach, in which the velocity and acceleration can be influenced by spatial coordinates of the individual. The time evolution of the state is described by ordinary or stochastic differential equations. Comprehensive reviews of these approaches and their advantages and disadvantages can also be found in Gazi(2004) [22] and Merrifield(2006) [23].

More recently, researchers have considered the use of bio-inspired behavior of landmarks from nature to find better and more inclusive solutions to the motion planning and control problems [24–26]. A landmark is a distinctive feature that exists naturally in the environment to support the motion. In the field of robotics, landmarks are either used for guidance to desired goal(s) [26–28], or to allow mapping and localization of robot positions [25,29,30]. A set of landmarks selected for a specific task is known as waypoints, which can also include physical ob-

* Corresponding author.
E-mail address: bibhya.sharma@usp.ac.fj (B. Sharma).

https://doi.org/10.1016/j.swevo.2021.100926
Received 13 August 2020; Received in revised form 2 June 2021; Accepted 4 June 2021
Available online 12 June 2021

jects, devices or coordinates imprinted with navigation details for robot navigation or human movements [24,31].

Moreover, landmarks for a planning problem are subgoals [32], and goals are landmarks [33] as well. Landmarks are abstract tasks that are mandatory and should be performed by any solution plan. Landmarks can be performed simultaneously, or they could be prioritized in hierarchical order. An example of hierarchical landmarks would be to complete task A before performing task B [34], where task B is to apply a finishing coat of paint to a building wall, and task A is to apply the undercoat to a building wall. In literature, a single robotic agent has been mostly considered for multiple point convergence. For instance, for a robot to navigate from starting position to the marked goal area, in [35], a robot converges to its goal using selected landmarks from several landmarks. Furthermore, Beinhofer *et. al.* [36] linearized the whole navigation cycle representing the landmark locations by a discrete set and then used a user-defined bound for the conservative approximation of landmark visibility and selection. The concepts of landmarks and waypoints have invariably been applied to multi-agents and robotic swarms in applications such as environmental tracking, sensor deployment, mine clearing, search-and-rescue, and intrusion detection [37–39], compounding the advantages of multiple robots with those of landmarks or waypoints.

This paper aims to develop the velocity controllers of a Lagrangian swarm of UGVs, which navigate via hierarchal landmarks to the swarm's target. The navigation of the swarm of UGVs will be based on the metaheuristic approach of Reynolds rules [40] which are (1) collision avoidance with neighbors, (2) matching velocity of the neighbors, and (3) staying close to the neighbors. The hierarchal landmarks serve as the waypoints for a swarm of UGVs. Navigation via the hierarchal landmarks requires different velocity controllers for the UGVs for each distinct landmark. Thus, navigating to a distinctive hierarchal landmark will give rise to a separate subsystem. Combining the distinct subsystems will, therefore, create a switched system. A switched system is a hybrid dynamical system comprising of a family of continuous-time subsystems and includes a law that coordinates the switching between them [41]. Therefore, the switched velocity controllers will enable the individuals of a swarm of UGVs to maneuver from their initial position in a *a priori* known environment via distinct hierarchal landmarks to their equilibrium state successfully. This approach is centered around significantly enhancing a technique of solving the find path problem for a swarm comprising of $n \in \mathbb{N}$ individuals developed by the authors in [42]. This novel technique can potentially have real-life applications in the military, health care, logistics, and surveillance. For instance, a sequence or series of hazardous or harmful areas to human beings can be mapped and sampled by a swarm of UGVs to determine the contamination. The authors constructed a planar Lagrangian swarm model based on the hypothesis that swarming is an interplay between long-range attraction and short-range repulsion between the individuals in the swarm. The stability of the switched system for the arbitrary switching signal is established by employing multiple Lyapunov functions. The velocity based-controllers for the individuals of a swarm of UGVs are derived for each subsystem using the multiple Lyapunov functions.

It is known that in measurements, there are rare, inconsistent observations with the largest part of the population of observations, called outliers. Noises and uncertainties can affect the convergence of the solution and its stability. Thus, the effects of noise will be later included in the velocity controllers to show its robustness.

The major contributions of this paper are:

1. Swarm navigation through hierarchal landmarks. In contrast, the swarm individuals in [37] navigated back and forth between two targets, whereas the swarm of robots in [39] explore an environment using multiple landmarks with limited sensor range.
2. The development of a new switched system from multiple Lyapunov functions for navigation.
3. Switched nonlinear, time-invariant, continuous and stabilizing velocity controllers of the individuals of a swarm of UGVs are distributed as it could be noted in the publications [22,43], the use of a gradient system ensures there is an element of distribution of tasks among the members of the swarm and that the swarm members are performing *distributed optimization*. Whereas there is no evidence of system stability present in [37] and [39].
4. The controllers' inherent robust nature due to LbCS absorbs the effect of noise and uncertainty and can exhibit different swarming patterns like split-and-rejoin, tunneling, and linear formations [14,42,44] while performing event-based hierarchal navigation. While the controllers presented in [42] only enable the swarm individuals to maneuver from their initial configuration to a goal configuration exhibiting self-organization patterns.

The paper's remainder is organized as follows: A literature review on the related work is presented in Section 2. Section 3 provides awareness of the LbCS. Section 4 gives a system for a swarm of UGVs. Section 5 provides an insight into our findpath problem via landmarks. The switched velocity-controllers for an individual of the swarm are derived from multiple Lyapunov functions in Section 6. In Section 6, the stability of the switch system is discussed vigorously. Section 7 provides an insight into the roles of parameters used in the multiple Lyapunov functions. In Sections 8, simulation studies of the UGVs are presented. The switched velocity controllers of the UGVs with the effect of noise are presented in Section 9, a discussion in Section 10. Finally, this paper is concluded with recommendations of future work in Section 11.

2. Related work

With the design of new mechanical systems and the growing list of real-life applications, there is still a sustained interest in finding feasible solutions to the problem of motion planning and control of robots which deal with coordinated, controlled, and collision-obstacle free movements in known, partially known, and unknown environments [2,45–47]. The advantage of the multi-agent system and swarm system is that such systems operate at a higher speed due to the parallel processing and proficiency in the relevant area of operation [48]. There is a need to find algorithms that present automated safe-smooth-short navigation in crowded and busy places such as malls, schools, colleges, universities, or industries. The new roles of companionship and assistance deal with precise and safe navigation in more constrained spaces. In literature, these solutions are secured from different techniques, strategies and methods usually categorised under two approaches; classical approach (including roadmap, cell decomposition, artificial potential field, virtual force field, graph theory, fuzzy logic), and more recently heuristic-based approach (including neural network, genetic algorithm, particle swarm optimization, ant-colony optimization, firefly algorithm, cuckoo search algorithm).

Existing research has demonstrated the effectiveness of fuzzy logic and artificial potential fields approach to provide a collision-free trajectory for a platoon of UGV [49,50]. The advantage of fuzzy logic systems is that it is a robust system where no precise inputs are required. The disadvantage of it is that these systems' accuracy is compromised as the system mostly works on inaccurate data and inputs. In comparison, the artificial potential fields method's advantages are its simplicity, easier implementation in practice, easier analytic representation of system singularities, limitations, and equalities. The major drawback of the artificial potential field approach is the possibility of getting trapped in the local minima. A popular method for path planning and obstacle avoidance is the Particle Swarm Optimisation (PSO) approach, which enables robots to escape local minima [51]. Communications and control structures in a group of UGV are theoretically established through the wide use of Graph theory [52,53]. Theoretically, graph search techniques are elegant, but they can involve computationally intensive algorithms.

For the past three decades, the entire focus has been on self-organization, scalability and robustness, formations, control and connectivity, path planning, and obstacle avoidance. Recently, the concepts of landmarks and waypoints have invariably been applied to multi-agents and robotic swarms in applications such as environmental tracking, sensor deployment, mine clearing, search-and-rescue, and intrusion detection [37–39], compounding the advantages of multiple robots with those of landmarks or waypoints. The navigation of swarm robots back and forth between two targets was studied in [37] via delay-tolerant wireless communications. Using the frontier-based exploration strategy, the bearing-based controller was designed for a swarm of robots with limited sensor range was presented in [39], which had to explore an environment with multiple landmarks. There is a need for controllers that could guide a swarm to its target destination using hierarchal landmarks.

The essence of the paper [42] was to provide Lyapunov-based controllers to $n \in \mathbb{N}$ individuals of a swarm. The controllers enabled the individuals to maneuver from their initial state to their equilibrium state autonomously. The system studied in [42] will be modified in this paper to meet the objective of this research.

3. Lyapunov-based control scheme

The multiple Lyapunov functions are derived from the Lyapunov-based Control Scheme (LbCS), which has been deployed successfully in literature to find feasible and stabilizing solutions for a wide spectrum of applications [1,2,14,42,45,54–56]. The Lyapunov-based Control Scheme falls under the artificial potential field method of the classical approach. The development of attractive and repulsive potential functions is the primary intention of LbCS. Subsequently, these functions are part of a total potential function called the Lyapunov function from which one could extract the time-invariant nonlinear velocity or acceleration-based controllers. Using LbCS, designing controllers is easy, and the controllers are continuous, which are the scheme's main strengths. It is easy to include control conditions, specifications, inequalities, and mechanical constraints of mechanical systems in the controllers through developing mathematical functions when applying LbCS [14,45,54–56]. The main disadvantage of LbCS is that algorithm singularities (local minima) can be introduced. In practical applications, continuity has to be discretized, and only asymptotic stability could be shown. The reader is referred to [14] for a detailed account of the LbCS.

An illustration of the LbCS is given utilizing Fig 1(a) and Fig 1(b). Fig 1(a) shows the contour plot generated over a workspace $-10 < z_1 < 150$ and $-10 < z_2 < 150$ for a robot whose initial position is at (10,10). The dashed line is the robot's trajectory from its initial position to its target position (100,100), which shows the robot avoids the obstacle positioned at (50,50) with a radius 10. Fig shows the 3D visualization of the attractive and repulsive potential fields. The blue line shows the Lyapunov function, which shows that the robot's energy is monotonically decreasing and is zero at the target position.

4. A Swarm of UGVs

Consider a swarm of $n \in \mathbb{N}$ individuals that we shall treat as rigid bodies [42]. In two-dimensional space, their translational components can describe the positions of the swarm individuals. Consider a swarm of $n \in \mathbb{N}$ UGV as car-like nonholonomic vehicle analyzed in [14].

4.1. Car-like UGV model

Let the position of the i^{th} UGV at time $t \geq 0$ be $\boldsymbol{x}_i = (x_i(t), y_i(t))$ with orientational angle $\theta_i = \theta_i(t)$, for all $i \in \{1, 2, 3, \dots, n\}$, with $(x_i(t_0), y_i(t_0)) =: (x_{i0}, y_{i0})$ and $\theta_i(t_0) = \theta_{i0}$ as initial conditions [42].

Definition 4.1. *The i^{th} rear wheel driven UGV with front wheel steering is a disk with radius r_{v_i} and is positioned at center (x_i, y_i) [42]. The i^{th} UGV is precisely described as the set*

$$V_i = \{(z_1, z_2) \in \mathbb{R}^2 : (z_1 - x_i)^2 + (z_2 - y_i)^2 \leq r_{v_i}^2\}. \tag{1}$$

Definition 4.2. *The centroid of the swarm of $n \in \mathbb{N}$ UGVs as mentioned in [42] is*

$$\boldsymbol{x}_C = (x_C, y_C) := \left(\frac{1}{n} \sum_{k=1}^{n} x_k, \frac{1}{n} \sum_{k=1}^{n} y_k \right). \tag{2}$$

The i^{th} rear wheel driven UGV with front wheel steering is shown in Fig. 2. The distance between the two axles is η and the length of each axel is l. Thus, the kinematic model, adopted from [1,2,14], of the i^{th} UGV with respect to its center $(x_i, y_i) \in \mathbb{R}^2$ is derived as

$$\left.\begin{aligned} \dot{x}_i &= v_i \cos\theta_i - \frac{\eta}{2} w_i \sin\theta_i, \\ \dot{y}_i &= v_i \sin\theta_i + \frac{\eta}{2} w_i \cos\theta_i, \\ \dot{\theta}_i &= w_i, \end{aligned}\right\} \tag{3}$$

where the variable θ_i gives the UGV's orientation with respect to the z_1-axis of the $z_1 z_2$ cartesian plane, and v_i and w_i are the translational and rotational velocities respectively. To ensure that the i^{th} UGV steers safely pass obstacles (either moving or static obstacles), we adopt the nomenclature of [2,14] and enclose the vehicle by the smallest possible circle. As shown in Fig. 2 the vehicle is enclosed by a protective circular region centered at (x_i, y_i), with radius $r_V := \dfrac{\sqrt{(2\epsilon_1 + \eta)^2 + (2\epsilon_2 + l)^2}}{2}$ where $\epsilon_1 > 0$ and $\epsilon_2 > 0$ are the clearance parameters. At $t \geq 0$, let $(\sigma_i(t), \psi_i(t)) := (x_i'(t), y_i'(t))$ be the instantaneous velocity of the i^{th} UGV. We have thus a system of first-order ODEs for the i^{th} UGV:

$$x_i'(t) = \sigma_i(t), \;\; y_i'(t) = \psi_i(t), \tag{4}$$

assuming the initial conditions at $t = t_0 \geq 0$ as $x_{i0} := x_i(t_0), \;\; y_{i0} := y_i(t_0)$. Suppressing t, we let $\mathbf{x}_i := (x_i, y_i) \in \mathbb{R}^2$, and $\mathbf{x} := (\mathbf{x}_1, \mathbf{x}_2, \mathbf{x}_3, \dots, \mathbf{x}_n) \in \mathbb{R}^{2n}$ be the state vectors. Also let

$\mathbf{x}_0 := \mathbf{x}(t_0) := (x_{10}, y_{10}, x_{20}, y_{20}, \dots, x_{n0}, y_{n0}) \in \mathbb{R}^{2n}$. If the instantaneous velocity (σ_i, ψ_i) has a state feedback law of the form

$$\sigma_i(t) := -\mu_i f_i(\mathbf{x}(t)),$$
$$\psi_i(t) := -\varphi_i g_i(\mathbf{x}(t)),$$

for $i \in \{1, 2, 3, \dots, n\}$, for some scalars μ_i, φ_i and some functions $f_i(\mathbf{x}(t))$, and $g_i(\mathbf{x}(t))$, to be constructed appropriately later, and if we define $\mathbf{g}_i(\mathbf{x}) := (-\mu_i f_i(\mathbf{x}), -\varphi_i g_i(\mathbf{x})) \in \mathbb{R}^2$ and $\mathbf{G}(\mathbf{x}) := (\mathbf{g}_1(\mathbf{x}), \dots, \mathbf{g}_n(\mathbf{x})) \in \mathbb{R}^{2n}$, then the swarm of n individuals is represented by

$$\dot{\mathbf{x}} = \mathbf{G}(\mathbf{x}), \;\; \mathbf{x}(t_0) = \mathbf{x}_0. \tag{5}$$

5. Findpath problem via landmarks for a swarm of UGVs

Considering *a priori* known workspace cluttered with $q \in \mathbb{N}$ stationary obstacles. Assume that the positions of the $m \in \mathbb{N}$ landmarks are prior known. System (5) has to go through each of these landmarks before going to its ultimate target, avoiding collision with static and moving obstacles.

Definition 5.1. *A landmark LM_p, $p = 1, 2, \cdots, m$, is a disk with center $\boldsymbol{x}_{LM_p} = (x_{LM_p}, y_{LM_p})$ and radius r_{LM_p}. It is described as the set*

$$LM_p = \{(z_1, z_2) \in \mathbb{R}^2 : (z_1 - x_{LM_p})^2 + (z_2 - y_{LM_p})^2 \leq r_{LM_p}^2\}. \tag{6}$$

Definition 5.2. *The k^{th} solid stationary obstacle is a disk with center$\boldsymbol{x}_{O_k} = (o_{k1}, o_{k2})$ and radius$r_{O_k} > 0$. It is described as the set*

$$O_k := \{(z_1, z_2) \in \mathbb{R}^2 : (z_1 - o_{k1})^2 + (z_2 - o_{k2})^2 \leq r_{O_k}^2\}. \tag{7}$$

Definition 5.3. *The ultimate target for the swarm of $n \in \mathbb{N}$ individuals is $\boldsymbol{x}_\tau$, which is actually a target for centroid of the swarm. It is a disk with center $\boldsymbol{x}_\tau = (a, b)$ and radius r_τ. It is described as the set*

$$\tau := \{(z_1, z_2) \in \mathbb{R}^2 : (z_1 - a)^2 + (z_2 - b)^2 \leq r_\tau^2\}. \tag{8}$$

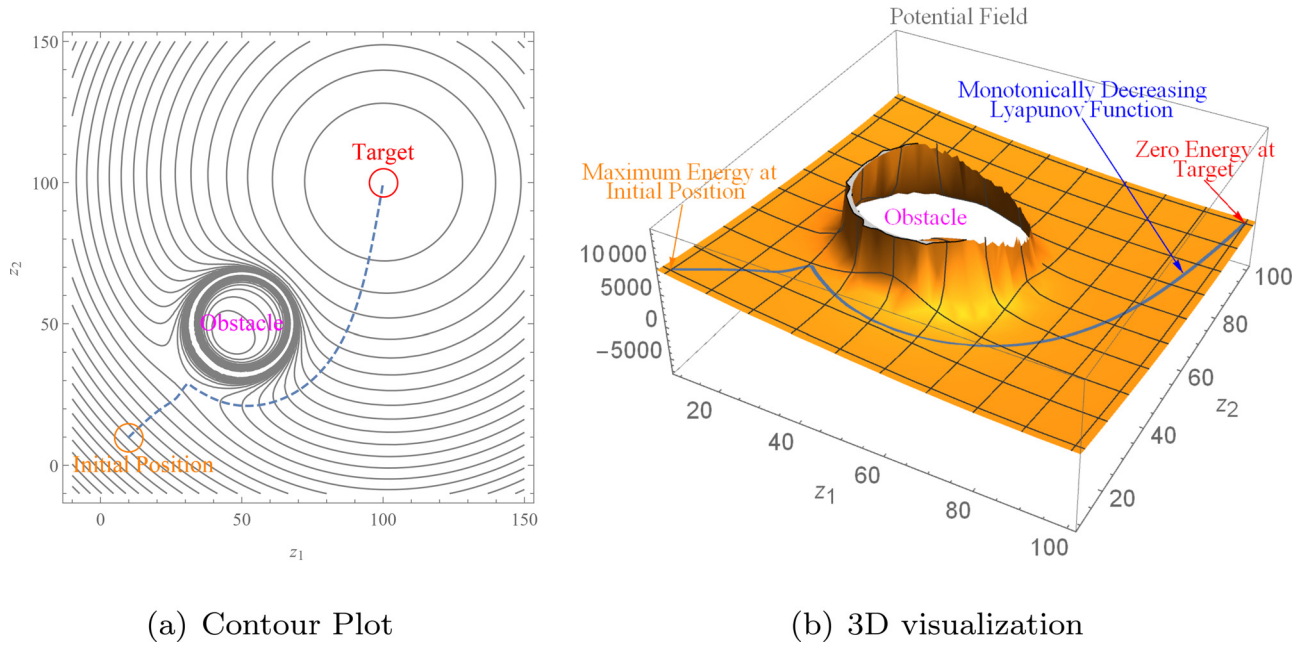

(a) Contour Plot (b) 3D visualization

Fig. 1. An illustration of the Lyapunov-based control scheme.

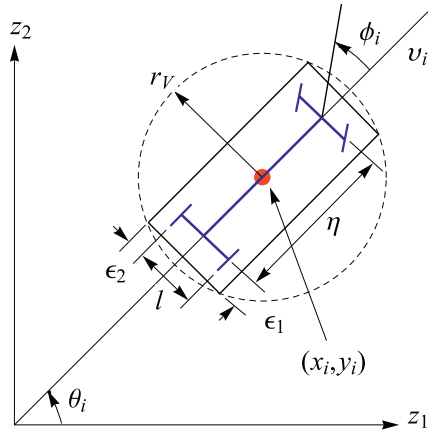

Fig. 2. Kinematic model of the i^{th} rear wheel driven UGV with front wheel steering and steering angle ϕ_i.

We can consider the target $\boldsymbol{x}_\tau$ as an additional landmark, that is, $LM_{m+1} = \tau$.

Definition 5.4. *The centroid of the swarm at time $t = 0$ is*

$$\boldsymbol{x}_{C_0} = (x_{C_0}, y_{C_0}) := \left(\frac{1}{n}\sum_{k=1}^{n} x_{k_0}, \frac{1}{n}\sum_{k=1}^{n} y_{k_0} \right). \tag{9}$$

The distance, d_{LM_p}, between the initial centroid (x_{C_0}, y_{C_0}) of the swarm and pth landmark, where $p \in \{1, 2, 3, \dots, m+1\}$, is given by

$$d_{LM_p} = \left\| \boldsymbol{x}_{C_0} - \boldsymbol{x}_{LM_p} \right\|. \tag{10}$$

It is further assumed that

$$d_{LM_1} < d_{LM_2} < d_{LM_3} < \dots < d_{LM_{m+1}}. \tag{11}$$

Then the equilibrium point for the i^{th} agent is $\mathbf{x}_{ie} = (x_{ie}, y_{ie}) \in \mathbb{R}^2$. If the system has an equilibrium point, we shall denote it by $\mathbf{x}_e = (\mathbf{x}_{1e}, \mathbf{x}_{2e}, \dots, \mathbf{x}_{ne}) = (x_{1e}, y_{1e}, x_{2e}, y_{2e}, \dots, x_{ne}, y_{ne}) \in \mathbb{R}^{2n}$.

6. Lyapunov-based velocity controllers of UGVS

6.1. Components of multiple Lyapunov function

In the multiple Lyapunov functions to be proposed, the following potential functions will be included.

6.1.1. Attraction to the centroid

The attractive potential function that will ensure that the i^{th} UGV is attracted towards the swarm centroid is proposed to be, for $i \in \{1, 2, 3, \dots, n\}$:

$$R_i(\mathbf{x}) := \frac{1}{2}\left[(x_i - x_C)^2 + \zeta (y_i - y_C)^2 \right]. \tag{12}$$

The control variable $\zeta \in \mathbb{R}$ determines the ratio of the minor axis (y-direction) to the major axis (x-direction) affecting the eccentricity of the swarm.

6.1.2. Landmark attraction function

The attractive potential function that will ensure that the centroid of system (5) maneuvers via landmarks to reach its target is proposed to be:

$$V_p(\mathbf{x}) := \frac{1}{2}\left\| \boldsymbol{x}_C - \boldsymbol{x}_{LM_p} \right\|^2. \tag{13}$$

6.1.3. Target attraction

To ensure that the UGVs converge to their equilibrium positions, we shall utilize the radically unbounded function about the target

$$H(\mathbf{x}) := \frac{1}{2}\left\| \boldsymbol{x}_C - \boldsymbol{x}_\tau \right\|^2. \tag{14}$$

6.1.4. Inter-agent collision avoidance

For short-range repulsion between the i^{th} and the j^{th} UGV, $j \neq i$, $i, j \in \{1, 2, 3, \dots n\}$, we consider the function

$$Q_{ij}(\mathbf{x}) := \frac{1}{2}\left[\left\| \boldsymbol{x}_i - \boldsymbol{x}_j \right\|^2 - (2r_{\upsilon_i})^2 \right]. \tag{15}$$

6.1.5. Stationary obstacle avoidance

For the purpose of avoiding possible collision with the k^{th} stationary solid obstacle governed by Eq. (7) where $i \in \{1, 2, 3, \dots, n\}$ and $k \in \{1, 2, 3, \dots, q\}$, we adopt the following obstacle avoidance function for the i^{th} UGV:

$$W_{ik}(\mathbf{x}) = \frac{1}{2}\left[\left\|\boldsymbol{x}_i - \boldsymbol{x}_{O_k}\right\|^2 - \left(r_{O_k} + r_{v_i}\right)^2\right]. \tag{16}$$

6.2. Multiple Lyapunov functions

Let there be real numbers α, δ_p, γ_i, β_{ij}, and λ_{ik}, and let $d = \left\|\boldsymbol{x}_C - \boldsymbol{x}_{C_0}\right\|$. Define, for $i, j \in \{1, 2, 3, \dots, n\}$ a family of Lyapunov function of the form,

$$\begin{aligned} L_p(\mathbf{x}) = {} & H(\mathbf{x})\left(\alpha + \delta_p V_p(\mathbf{x}) + \sum_{i=1}^{n}\left(\gamma_i R_i(\mathbf{x}) + \sum_{\substack{j=1,\\ j\neq i}}^{n}\frac{\beta_{ij}}{Q_{ij}(\mathbf{x})}\right)\right) \\ & + H(\mathbf{x})\sum_{i=1}^{n}\sum_{k=1}^{q}\frac{\lambda_{ik}}{W_{ik}(\mathbf{x})} \end{aligned} \tag{17}$$

which we invoke according to the switching rule

$$p = \begin{cases} 1, & 0 \le d < d_{LM_1} \\ 2, & d_{LM_1} \le d < d_{LM_2} \\ 3, & d_{LM_2} \le d < d_{LM_3} \\ \vdots & \\ m+1, & d_{LM_m} \le d \le d_{LM_{m+1}}. \end{cases} \tag{18}$$

6.3. Velocity controllers

Along a trajectory of system (5), we have

$$\dot{L}_p(\mathbf{x}) = \sum_{i=1}^{n}\left[f_{i_p}(\mathbf{x})\dot{x}_i + g_{i_p}(\mathbf{x})\dot{y}_i\right], \tag{19}$$

where

$$\begin{aligned} f_{i_p}(\mathbf{x}) = {} & \frac{1}{n}(x_C - a)\left(\alpha + \delta_p V_p(\mathbf{x}) + \gamma_i R_i(\mathbf{x}) + \sum_{\substack{j=1,\\ j\neq i}}^{n}\frac{\beta_{ij}}{Q_{ij}(\mathbf{x})} + \sum_{k=1}^{q}\frac{\lambda_{ik}}{W_{ik}(\mathbf{x})}\right) \\ & + H(\mathbf{x})\left(\frac{\delta_p}{n}\left(x_C - x_{LM_p}\right) + \gamma_i(x_i - x_C)\right) \\ & - H(\mathbf{x})\left(2\sum_{\substack{j=1,\\ j\neq i}}^{n}\frac{\beta_{ij}}{Q_{ij}^2(\mathbf{x})}(x_i - x_j) + \sum_{k=1}^{q}\frac{\lambda_{ik}}{W_{ik}^2(\mathbf{x})}(x_i - o_{k1})\right) \end{aligned} \tag{20}$$

and

$$\begin{aligned} g_{i_p}(\mathbf{x}) = {} & \frac{1}{n}(y_C - b)\left(\alpha + \delta_p V_p(\mathbf{x}) + \gamma_i R_i(\mathbf{x}) + \sum_{\substack{j=1,\\ j\neq i}}^{n}\frac{\beta_{ij}}{Q_{ij}(\mathbf{x})} + \sum_{k=1}^{q}\frac{\lambda_{ik}}{W_{ik}(\mathbf{x})}\right) \\ & + H(\mathbf{x})\left(\frac{\delta_p}{n}\left(y_C - y_{LM_p}\right) + \gamma_i(y_i - y_C)\right) \\ & - H(\mathbf{x})\left(2\sum_{\substack{j=1,\\ j\neq i}}^{n}\frac{\beta_{ij}}{Q_{ij}^2(\mathbf{x})}(y_i - y_j) + \sum_{k=1}^{q}\frac{\lambda_{ik}}{W_{ik}^2(\mathbf{x})}(y_i - o_{k2})\right). \end{aligned} \tag{21}$$

Let there be scalars $\mu_i > 0$ and $\varphi_i > 0$. Then the velocity controllers of system (5) are

$$\sigma_i = -\mu_i f_{i_p} \text{ and } \psi_i = -\varphi_i g_{i_p}. \tag{22}$$

Given (22), system (5) becomes therefore a switched system

$$\dot{\mathbf{x}} = \mathbf{G}_p(\mathbf{x}), \quad \mathbf{x}_0 := \mathbf{x}(t_0), \quad p \in \{1, 2, \cdots, m+1\}. \tag{23}$$

6.3.1. Steering control laws

The steering control laws could be accordingly defined as

$$\left.\begin{aligned} v_i &:= -\kappa_i\left(f_{i_p}(\mathbf{x})\cos\theta_i + g_{i_p}(\mathbf{x})\sin\theta_i\right), \\ w_i &:= \frac{2\kappa_i}{\eta}\left(f_{i_p}(\mathbf{x})\sin\theta_i - g_{i_p}(\mathbf{x})\cos\theta_i\right), \end{aligned}\right\} \tag{24}$$

where κ_i is desired to be some arbitrary continuous positive function of x_i and y_i and $f_{i_p}(\mathbf{x})$ and $g_{i_p}(\mathbf{x})$ are defined in (20) and (21) respectively. Thus, system (3) can be expressed as

$$\left.\begin{aligned} \dot{x}_i &= -\kappa_i f_{i_p}(\mathbf{x}), \\ \dot{y}_i &= -\kappa_i g_{i_p}(\mathbf{x}), \\ \dot{\theta}_i &= \frac{2\kappa_i}{\eta}\left(f_{i_p}(\mathbf{x})\sin\theta_i - g_{i_p}(\mathbf{x})\cos\theta_i\right). \end{aligned}\right\} \tag{25}$$

The positions of the vehicles $\left(x_i(t), y_i(t)\right)$ are governed by first two terms of (25) while the third governs their orientations.

6.3.2. Maximum velocities

Practically there are restrictions on the velocities and steering angle of a vehicle. A vital role is performed by the function $\kappa_i = \kappa_i(x_i, y_i) > 0$ in restricting the magnitudes of v_i, w_i and the steering angles ϕ_i.

Given any real number $\chi > 0$, from (24),

$$\left.\begin{aligned} |v_i| &\le \kappa_i\left(\chi + \left|f_{i_p}(\mathbf{x})\right| + \left|g_{i_p}(\mathbf{x})\right|\right), \\ |w_i| &\le \frac{2\kappa_i}{\eta}\left(\chi + \left|f_{i_p}(\mathbf{x})\right| + \left|g_{i_p}(\mathbf{x})\right|\right). \end{aligned}\right\} \tag{26}$$

If we let $v_{max} := \max_{i\in\mathbb{N}}|v_i|$ be the maximum translational speed then from the first inequality of (26)

$$\kappa_i := \frac{v_{\max}}{\chi + \left|f_{i_p}(\mathbf{x})\right| + \left|g_{i_p}(\mathbf{x})\right|}. \tag{27}$$

6.3.3. Maximum steering angle

The size of steering angle ϕ_i is restricted using (26) and (27). Let the maximum steering angle be $\phi_{max} := \max_{i\in\mathbb{N}}|\phi_i|$, where $0 < \phi_{max} < \frac{\pi}{2}$. Then

$$|v_i| \le v_{\max} \text{ and } {v_i}^2 \ge \rho^2 {w_i}^2 \text{ where } \rho := \frac{\eta}{\tan\phi_{\max}} \tag{28}$$

are the constraints imposed on the translational velocities, v_i, and the rotational velocities w_i as shown in [57]. From (28)

$$|w_i| \le \left|\frac{v_i}{\rho}\right| \le \frac{v_{\max}}{|\rho|}. \tag{29}$$

From (26), (27) and (29)

$$|w_i| \le \frac{2\kappa_i}{\eta}\left(\chi + \left|f_{i_p}(\mathbf{x})\right| + \left|g_{i_p}(\mathbf{x})\right|\right)$$

and

$$|w_i| \le \frac{v_{\max}}{|\rho|}\left(\chi + \left|f_{i_p}(\mathbf{x})\right| + \left|g_{i_p}(\mathbf{x})\right|\right).$$

Let $|\rho| = \frac{\eta}{2}$ and from (28) $\tan\phi_{max} = 2$. Thus $\phi_{max} = \tan^{-1}2$ and hence the maximum steering angle of every vehicle is set at $\phi_{max} = \tan^{-1}2$. To add on, maximum velocity and maximum steering angle of a car-like vehicle can also be treated as artificial constraints, which could be part of the total potential as repulsive potentials. The above technique is equivalent.

6.4. Stability analysis

It is evident that $L_p(\mathbf{x})$, for $p = \{1, 2, \cdots, m+1\}$, is positive over the domain

$$D\big(L_p(\mathbf{x})\big) := \Big\{\mathbf{x} \in \mathbb{R}^{2n} : Q_{ij}(\mathbf{x}) > 0, W_{ik}(\mathbf{x}) > 0,\ \forall\, i, j = \{1, 2, 3, \dots, n\}, \\ i \neq j \text{ and } k = \{1, 2, 3, \dots, q\}\Big\}.$$

With respect to system (3) and with the control laws (24),

$$\dot{L}_p(\mathbf{x}) = -\sum_{i=1}^{n} \frac{1}{\kappa_i}\left(v_i{}^2 + \frac{\eta^2}{4} w_i{}^2\right) \leq 0,$$

$\forall \mathbf{x} \in D\big(L_p(\mathbf{x})\big)$. At the target, where $(x_C, y_C) = (a, b)$, the instantaneous velocities, σ_i and ψ_i, are zero because $f_{i_p} = 0$ and $g_{i_p} = 0$. Thus, the individuals assume a constant configuration or arrangement about the target. Their stationary positions therefore are components of an equilibrium point $\mathbf{x}_e$ of system (23). It is easy to see that $L_p(\mathbf{x}_e) = 0$, $L_p(\mathbf{x}) > 0\ \forall\ \mathbf{x} \neq \mathbf{x}_e$ and $\dot{L}_p(\mathbf{x}) \leq 0$. System (23) has the simple switching sequence $S = (x_0, y_0) : (p_0, t_0), (p_1, t_1)$ for $p = 1, \dots, m+1$, from which we easily get the trajectory

$$\mathbf{x}_S(\cdot) := \Big\{(p_0, t_0) : \dot{\mathbf{x}} = \mathbf{G}_{p_0}(\mathbf{x}(t), t),\quad p = 1, \dots, m+1,\ t_0 \leq t < t_1\Big\}.$$

Thus, $L_p(\mathbf{x})$ are monotonically non-increasing on $\mathcal{I}(S|p)$. Hence, for S and for all p, L_p are Lyapunov-like for $\mathbf{G}_p$ and $\mathbf{x}_S(\cdot)$ over $S|p$. Accordingly, by Branicky's Theorem 2.3 [58], system (23) is stable in the sense of Lyapunov. Looking at equations (20) and (21), we see that the functions that appear in the denominator are Q_{ij}, for all $j \neq i$, $i, j \in \{1, 2, 3, \dots, n\}$ and W_{ik} for $i \in \{1, 2, 3, \dots, n\}$ and $k \in \{1, 2, 3, \dots, q\}$. Hence, we can easily conclude that $\mathbf{G}_p(\mathbf{x}) \in C^1[D(L_p(\mathbf{x})), (\mathbb{R})^2]$ for all $p = \{1, 2, \cdots, m+1\}$, which implies that at least on some time interval $[t_0, s]$, $s > 0$, the solution of $\mathbf{x}(t)$ of system (23) exists and is in $D(L_p(\mathbf{x}))$. Certainly, since the functions Q_{ij} and W_{ik} appear in the denominator in (20) and (21), they will also appear in the denominator of higher-order partial derivatives, with each derivative continuous on $D(L_p(\mathbf{x}))$. This indicates that indeed $\mathbf{G}_p(\mathbf{x}) = (-\mu_i f_{i_p}(\mathbf{x}), -\varphi_i g_{i_p}(\mathbf{x})) \in C^\infty[D(L_p(\mathbf{x})), \mathbb{R}^2]$. This implies the existence of the solution $\mathbf{x}(t)$ of system (23) on $[t_0, s+\rho]$, $\rho > 0$ being independent of $s > 0$. Hence, we can conclude that $\mathbf{G}_p(\mathbf{x})$ is globally Lipschitz continuous on $D(L_p(\mathbf{x}))$. Therefore, system (23) is stable for a swarm of $n \in \mathbb{N}$ individuals for hierarchal landmark navigation.

7. Roles of the parameters in the Lyapunov function

In this section, we provide an overview of the roles of the parameters. This is an altered strategy from work conducted in [2,14,44,54]. Consider our multiple Lyapunov functions (18) again

$$L_p(\mathbf{x}) = H(\mathbf{x})\left(\alpha + \delta_p V_p(\mathbf{x}) + \sum_{i=1}^{n}\left(\gamma_i R_i(\mathbf{x}) + \sum_{\substack{j=1,\\ j\neq i}}^{n} \frac{\beta_{ij}}{Q_{ij}(\mathbf{x})}\right)\right) \\ + H(\mathbf{x}) \sum_{i=1}^{n}\sum_{k=1}^{q} \frac{\lambda_{ik}}{W_{ik}(\mathbf{x})}$$

which we invoke according to the switching rule

$$p = \begin{cases} 1, & 0 \leq d < d_{LM_1} \\ 2, & d_{LM_1} \leq d < d_{LM_2} \\ 3, & d_{LM_2} \leq d < d_{LM_3} \\ \vdots & \\ m+1, & d_{LM_m} \leq d \leq d_{LM_{m+1}}. \end{cases}$$

The parameter $\alpha > 0$ can be considered as a measurement of the strength of attraction between the swarm centroid $\boldsymbol{x}_C$ and the ultimate swarm target. The smaller the parameter is, the slower the convergence of the swarm centroid to the swarm target. Hence, α can be called a *target convergence parameter*. The parameter δ_p invoke according to the switching rule (18) can be considered as a measurement of the strength of attraction between the swarm centroid $\boldsymbol{x}_C$ and the p^{th} landmark. The smaller the parameter is, the slower the swarm centroid's convergence to the p^{th} landmark. Hence, δ_p can be called the *landmark convergence parameter*. At large distances between the i^{th} and the j^{th} individuals, the ratio,

$$\sum_{i=1}^{n}\sum_{\substack{j=1,\\ j\neq i}}^{n} \frac{\beta_{ij}}{Q_{ij}(\mathbf{x})} T(\mathbf{x}) \tag{30}$$

is negligible, and the term $\sum_{i=1}^{n} \gamma_i R_i(\mathbf{x}) T(\mathbf{x})$ dominates and acts as the *attraction function*; each individual is attracted to the centroid. Thus, the parameter $\gamma_i > 0$ can be considered as a measurement of the strength of attraction between an individual i and the swarm centroid $\boldsymbol{x}_C$. The smaller the parameter is, the weaker the cohesion of the swarm is. Hence, γ_i can be called a *cohesion parameters*. Now, consider the situation where any two individuals i and j approach each other. In this case, Q_{ij} decreases, and the ratio (30) increases, with $\beta_{ij} > 0$ acting as a *coupling parameters* that is a measurement of the strength of interaction between the individuals. In this way, the ratio (30) acts as an *inter-individual collision-avoidance function* because it can be allowed to increase in value (corresponding to avoidance) as individuals approach each other. The parameter λ_{ik} is the *stationary obstacle avoidance* parameter, respectively. We have used two other parameters, $\mu_i > 0$, and $\varphi_i > 0$ in system (23). Because the parameters are a measure of the rate of decrease of $L_p(t)$ at time $t > 0$, we name them *convergence parameters*.

8. Simulation results

Simulations were generated using Wolfram Mathematica 11.2 software. To achieve the desired results, a number of sequential Mathematica commands were executed. Before the algorithm is executed, the values of the convergence, cohesion, coupling, and stationary obstacle avoidance parameters have to be stated. The number and positions of the hierarchal landmarks, number of obstacles, and UGVs have to be defined. We numerically simulated system (25) using the RK4 method (Runge-Kutta Method) and the following values for each car-like vehicle.

- **Clearance parameters:** $\epsilon_1 = \epsilon_2 = 0.1$;
- **Width and length of the vehicle:** $l = 1$, $\eta = 2$;
- **Radius of circular protective region:** $r = 1.25$;
- **Maximum speeds and steering angle:** $v_{max} = 1$ and $\phi_{max} = \tan^{-1} 2$;
- $\chi = 1$ in κ_i defined as in (27).

At $t = 0$, the initial positions $(x_{i0}(0), y_{i0}(0))$ and orientations $\theta_i(0)$ were randomly generated. The initial velocities are calculated from these values from (24). The vehicles are drawn as arrows, with the arrowhead indicating the front of the vehicles.

Due to the inherent nature of the artificial potential field method, which includes LbCS, there is a possibility that some initial conditions can produce trajectories that get trapped in local minima. Such initial conditions are avoided when assigning values to parameters through brute-force.

Example 8.1. Navigation via Landmark in Obstacle Free Configuration Space

We consider a swarm of 10 UGVs with 3 landmarks. The initial positions and orientations of UGVs are shown in small orange circles as shown in Fig 3. The swarm clusters around the centroid as time evolves, and then it moves to the target of the centroid as a well-spaced the cohesive group as shown in Fig 3. Fig 4 shows that $L_p(\mathbf{x})$ decreases on each interval where the p^{th} subsystem is active. This indicates that the swarm

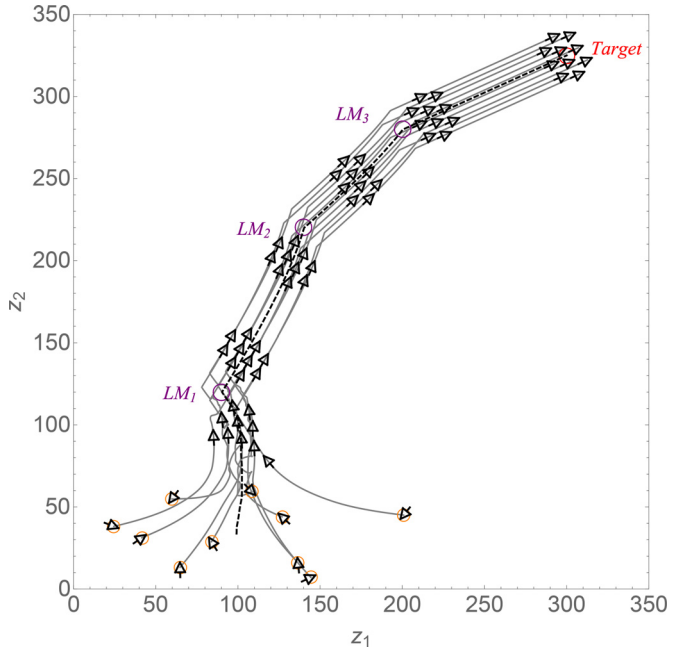

Fig. 3. *Example 8.1*. Positions and orientations of UGVs at $t = 0, 118, 205, 290, 380, 465$ and 600 respectively show the self-organization of the UGVs. The trajectory of the centroid is shown in dashed. For this formation, $\alpha = 0.000001$, $\gamma_i = 0.1$, $\beta_{ij} = 10$, $\delta_p = 0.2$ for $p \in \{1, 2, 3, 4\}$ and $\zeta = 1$.

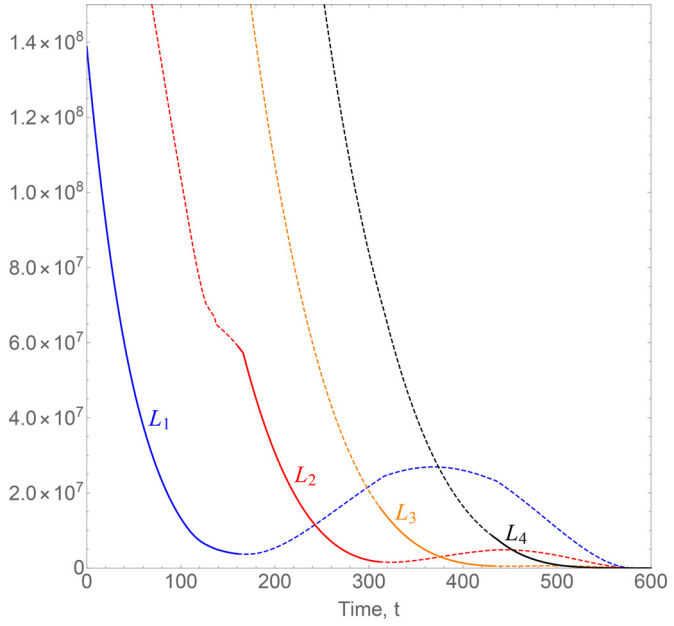

Fig. 4. *Example 8.1*. Multiple Lyapunov-like functions. Solid/dashed denotes corresponding system active/inactive.

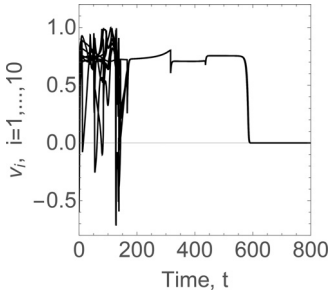

Fig. 5. *Example 8.1*. The instantaneous velocities of the agents showing rapid deceleration as the swarm approaches the target.

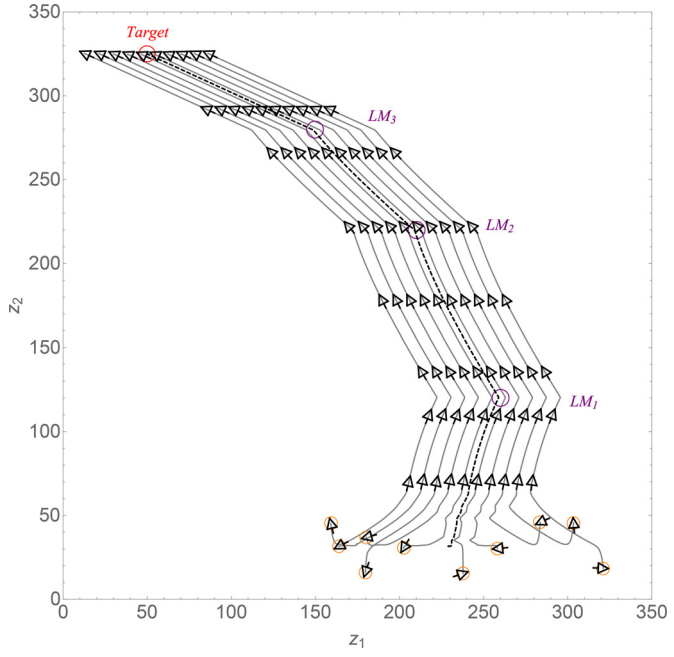

Fig. 6. *Example 8.2*. Positions and orientations of UGVs at $t = 0, 97, 149, 189, 255, 319, 409, 473$ and 800 respectively show the self-organization of the UGVs. The trajectory of the centroid is shown in dashed. For this formation, $\alpha = 0.000001$, $\gamma_i = 0.1$, $\beta_{ij} = 10$, $\delta_p = 0.2$ for $p \in \{1, 2, 3, 4\}$ and $\zeta = 60$.

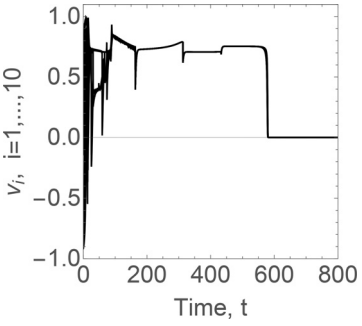

Fig. 7. Example 8.2. The instantaneous velocities of the agents showing rapid deceleration as the swarm approaches the target.

is converging to its target. The vehicles' velocities are captured in Fig 5, which shows that the swarm is a cohesive group since the individual velocities are the same as time evolves.

Example 8.2 (Linear Formation)**.** A swarm to take up linear formation is of very high importance, as mentioned in [5], as this formation could be utilized to search extensive areas such as exclusive economic zone (EEZ) for search and rescue. The linear formation is designed using the control variable ζ given in equation (12). If ζ is significantly small, it will position the swarm individuals in a vertical linear formation. However, if ζ is significantly large, it will position the swarm individuals in a horizontal linear formation. In this example, a swarm of 10 UGVs is considered. The initial positions and orientations of UGVs are shown in small orange circles as shown in Fig. 6. The swarm clusters around the centroid as time evolves, and it moves to the target of the centroid via the landmarks in a linear formation as a well-spaced cohesive group as shown in Fig. 6. The velocities of the vehicles are captured in Fig 7, which shows that the swarm is a cohesive group since the individual velocities are the same as time evolves.

Example 8.3 Navigation via Landmark in an Obstacle-Cluttered Environment. A swarm of 10 UGVs clusters around the centroid as time evolves and then moves to the centroid's target as a well-spaced cohe-

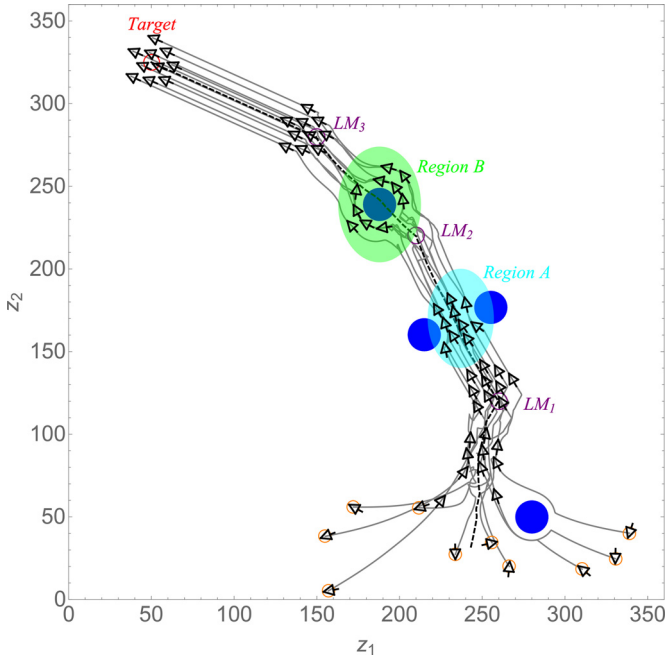

Fig. 8. Example 8.3. Position and orientation of the UGVs at $t = 0, 124, 214, 276, 411, 500$ and 800 respectively. The trajectory of (x_C, y_C) is shown in dashed. For this formation, $\alpha = 0.000001$, $\gamma_i = 0.1$, $\lambda_{ik} = \beta_{ij} = 10$, $\delta_p = 0.2$ for $p \in \{1, 2, 3, 4\}$ and $\zeta = 1$.

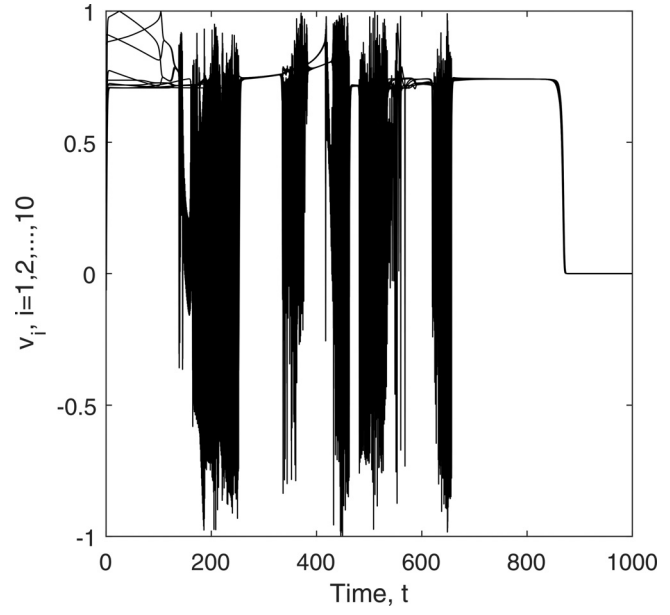

Fig. 9. Example 8.3. The instantaneous velocities of the agents showing rapid deceleration as the swarm approaches the target.

sive group avoiding obstacles in its path, as shown in Fig. 8. A split-and-rejoin and the tunneling maneuvers are emerging, as shown in Region A and Region B, respectively. A split-and-rejoin maneuver is where the swarm individuals move cohesively together in a formation split to steer past the encountering obstacle(s) and then rejoin. Moreover, tunneling maneuver is where the swarm individuals change formation to drive past narrow passageways. The vehicles' velocities are shown in Fig 9, which shows that the swarm is a cohesive group since the individual velocities are the same as time evolves.

9. Effect of noise

In this section, the effect of noise on the controllers is considered. The noise components are included in the obstacle avoidance functions, and the multiple Lyapunov functions are redefined as follows

$$L_p(\mathbf{x}) = H(\mathbf{x})\left(\alpha + \delta_p V_p(\mathbf{x}) + \sum_{i=1}^{n}\left(\gamma_i R_i(\mathbf{x}) + \sum_{\substack{j=1,\\ j\neq i}}^{n}\frac{\beta_{ij}}{Q_{ij}(\mathbf{x}) + \xi\varpi_{ij}}\right)\right) + H(\mathbf{x})\sum_{i=1}^{n}\sum_{k=1}^{q}\frac{\lambda_{ik}}{W_{ik}(\mathbf{x}) + \xi\varrho_{ik}} \tag{31}$$

which is invoked according to the switching rule

$$p = \begin{cases} 1, & 0 \le d < d_{LM_1} \\ 2, & d_{LM_1} \le d < d_{LM_2} \\ 3, & d_{LM_2} \le d < d_{LM_3} \\ \vdots & \\ m+1, & d_{LM_m} \le d \le d_{LM_{m+1}}. \end{cases} \tag{32}$$

The terms ϖ_{ij} and ϱ_{ik} are time-dependent variables randomized between and including -1 and 1 and $\xi \in [0, 1]$ is the noise level. Thus, the functions $f_{i_p}(\mathbf{x})$ and $g_{i_p}(\mathbf{x})$ in the velocity controllers of system (5) as showed in equation (22) with effect of noise would be

$$\begin{aligned} f_{i_p}(\mathbf{x}) = {} & \frac{1}{n}(x_C - a)\left(\alpha + \delta_p V_p(\mathbf{x}) + \gamma_i R_i(\mathbf{x}) + \sum_{\substack{j=1,\\ j\neq i}}^{n}\frac{\beta_{ij}}{Q_{ij}(\mathbf{x}) + \xi\varpi_{ij}}\right) \\ & + \frac{1}{n}(x_C - a)\sum_{k=1}^{q}\frac{\lambda_{ik}}{W_{ik}(\mathbf{x}) + \xi\varrho_{ik}} \\ & + H(\mathbf{x})\left(\frac{\delta_p}{n}\left(x_C - x_{LM_p}\right) + \gamma_i(x_i - x_C)\right) \\ & - 2H(\mathbf{x})\sum_{\substack{j=1,\\ j\neq i}}^{n}\frac{\beta_{ij}}{\left(Q_{ij}(\mathbf{x}) + \xi\varpi_{ij}\right)^2}(x_i - x_j) \\ & - H(\mathbf{x})\sum_{k=1}^{q}\frac{\lambda_{ik}}{\left(W_{ik}(\mathbf{x}) + \xi\varrho_{ik}\right)^2}(x_i - o_{k1}) \end{aligned} \tag{33}$$

and

$$\begin{aligned} g_{i_p}(\mathbf{x}) = {} & \frac{1}{n}(y_C - b)\left(\alpha + \delta_p V_p(\mathbf{x}) + \gamma_i R_i(\mathbf{x}) + \sum_{\substack{j=1,\\ j\neq i}}^{n}\frac{\beta_{ij}}{Q_{ij}(\mathbf{x}) + \xi\varpi_{ij}}\right) \\ & + \frac{1}{n}(y_C - b)\sum_{k=1}^{q}\frac{\lambda_{ik}}{W_{ik}(\mathbf{x}) + \xi\varrho_{ik}} \\ & + H(\mathbf{x})\left(\frac{\delta_p}{n}\left(y_C - y_{LM_p}\right) + \gamma_i(y_i - y_C)\right) \\ & - 2H(\mathbf{x})\sum_{\substack{j=1,\\ j\neq i}}^{n}\frac{\beta_{ij}}{\left(Q_{ij}(\mathbf{x}) + \xi\varpi_{ij}\right)^2}(y_i - y_j) \\ & - H(\mathbf{x})\sum_{k=1}^{q}\frac{\lambda_{ik}}{\left(W_{ik}(\mathbf{x}) + \xi\varrho_{ik}\right)^2}(y_i - o_{k2}) \end{aligned} \tag{34}$$

respectively.

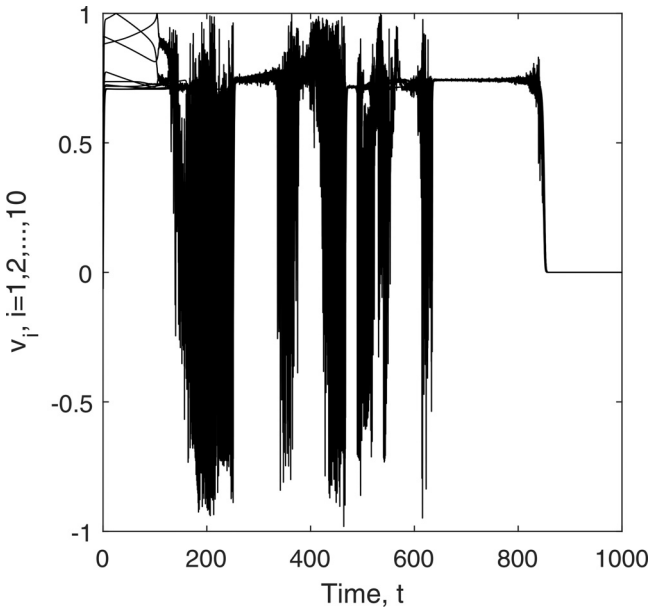

Fig. 10. *Example 9.1*. The instantaneous velocities of the agents with $\xi = 0.5$. as the swarm approaches the target.

9.1. Stability analysis

Subsection 6.4 is followed with the fact that at the target, where $(x_C, y_C) = (a, b)$, the instantaneous velocities, σ_i and ψ_i, are zero because f_{i_p} and g_{i_p} are zero, in Eqs. (33) and (34), respectively.

9.2. Simulation result

Example 9.1. For Example 8.3 with the same parameters the velocities of the vehicles with noise level $\xi = 0$ and $\xi = 0.5$ are shown in Fig 9 and Fig 10, respectively.

10. Discussion

The switched nonlinear, time-invariant, continuous, and stabilizing velocity controllers of the individuals of a swarm of UGVs, that exhibit self-organization patterns for navigation through hierarchal landmarks have been established. Simulation results such as the ones shown in Fig 3, Fig 6, and Fig 8 show the controllers' effectiveness in navigation via hierarchal landmarks. It is evident, as seen in Fig 10 that the controllers presented can absorb the effect of noise and uncertainty, which invariably show the robustness of the system.

In comparison to the systems presented in [37] and [39] our system is stable; exhibits emergent patterns; absorbs the effect of noise, shows system robustness, and most importantly, can navigate via hierarchal landmarks, whereas the system presented in [42] cannot.

Although we have this component of distributed optimization as the individual velocities are discovered, our approach doesn't guarantee scalability. Any expansion in swarm size brings about a more prominent interest in computing resources. In applied circumstances, for detecting abilities, each individual knows the situation of all other individuals in the swarm. In any case, the dramatic growth in processing power, memory, and storage capacity of computing gadgets joined by diminishing costs of these gadgets, and the expanding utilization of the Global Positioning System to counterbalance detecting constraints will assume a significant part in lessening the effect of scaling. Besides, after the presentation of quantum computing, scalability will not be an issue by any stretch of the imagination [44].

11. Conclusion

While the control of a swarm of UGVs is a well studied problem, this paper presents a new and novel solution where a Lagrangian swarm of UGVs is navigated to its target via hierarchal landmarks in cluttered environment using nonlinear time-invariant continuous velocity-based control laws derived from LbCS. The switched velocities of the swarm individuals were constructed using multiple Lyapunov functions that gave rise to a switched system. Interaction of the three main pillars of LbCS, which are safety, shortness, and smoothest path for motion planning, bring about cost and time effectiveness and efficiency of the velocity controllers. The switched system was successfully showed to be stable in the sense of Lyapunov. Moreover, linear formation, split-and-rejoin, and tunneling maneuvers emergent due to individuals' self-organization of the swarm of UGVs. The effect of noise on velocity controllers was presented to exhibit the system's robustness. The drawback of this approach is that scalability is not guaranteed. Future work could be of developing a system in which the roles of the landmark are dynamic.

Declaration of Competing Interest

The authors declare that they have no known competing financial interests or personal relationships that could have appeared to influence the work reported in this paper.

CRediT authorship contribution statement

Sandeep A. Kumar: Conceptualization, Methodology, Writing - original draft. **B. Sharma:** Methodology, Writing - review & editing. **J. Vanualailai:** Methodology, Validation, Writing - review & editing. **A. Prasad:** Validation, Writing - review & editing.

References

[1] B. Sharma, J. Vanualailai, S. Singh, Motion planning and posture control of multiple n-link doubly nonholonomic manipulators, Robotica 35 (2015) 1–25, doi:10.1017/S0263574714002604.
[2] B. Sharma, J. Raj, J. Vanualailai, Navigation of carlike robots in an extended dynamic environment with swarm avoidance., Int. J. Robust Nonlinear Control 28 (2018) 678–698.
[3] A. Filipescu, V. Minzu, A. Filipescu, E. Minca, Advances in Automation and Robotics, Vol.1. Lecture Notes in Electrical Engineering, Springer, pp. 401–409.
[4] C. Pacchierotti, S. Sinclair, M. Solazzi, A. Frisoli, V. Hayward, D. Prattichizzo, Wearable haptic systems for the fingertip and the hand: taxonomy, review, and perspectives, IEEE Trans Haptics 10 (4) (2017) 580–600.
[5] S.A. Kumar, J. Vanualailai, A Lagrangian UAV swarm formation suitable for monitoring exclusive economic zone and for search and rescue, in: Proceedings of the 2017 IEEE Conference on Control Technology and Applications, Kohala Coast, Hawai'i, USA, 2017, pp. 1874–1879.
[6] K. Shojaei, Neural adaptive output feedback formation control of type (m, s) wheeled mobile robots, Int. J. Adapt. Control Signal Process 29 (2015) 855–876.
[7] X. Xing, R. Zhou, L. Yang, The current status of development of pedestrian autonomous navigation technology, in: Proceedings of the 26th Saint Petersburg International Conference on Integrated Navigation Systems (ICINS), 2019.
[8] K.M. Williams, M.H. Assaf, Intelligent public transportation system, International Journal of Mathematics and Computers in Simulation 112 (2018) 124–132.
[9] A. Prasad, B. Sharma, J. Vanualailai, S.A. Kumar, A geometric approach to target convergence and obstacle avoidance of a nonstandard tractor-trailer robot, Int. J. Robust Nonlinear Control 30 (13) (2020) 4924–4943, doi:10.1002/rnc.5021.
[10] A. Prasad, B. Sharma, J. Vanualailai, A solution to the motion planning and control problem of a car-like robot via a single layer perceptron, Robotica 32 (6) (2014) 935–952.
[11] S.A. Kumar, J. Vanualailai, B. Sharma, Lyapunov functions for a planar swarm model with application to nonholonomic planar vehicles, in: Proceedings of the 2015 IEEE Conference on Control Applications, IEEE, Sydney, Australia, 2015, pp. 1919–1924.
[12] S.A. Kumar, J. Vanualailai, B. Sharma, A. Chaudary, V. Kapadia, Emergent formations of a Lagrangian swarm of unmanned ground vehicles, in: Proceedings of the 2016 14th International Conference on Control, Automation, Robotics and Vision, ICARCV 2016, IEEE, Phuket, Thailand, 2016.
[13] A. Devi, J. Vanualailai, S.A. Kumar, B. Sharma, A cohesive and well-spaced swarm with application to unmanned aerial vehicles, in: Proceedings of the 2015 2017 International Conference on Unmanned Aircraft Systems (ICUAS), IEEE, Miami, FL, USA, 2017, pp. 698–705.
[14] B. Sharma, J. Vanualailai, S. Singh, Tunnel passing maneuvers of prescribed formations, Int. J. Robust Nonlinear Control 24 (5) (2014) 876–901.

[15] A. Khan, Y. Anwar, Advances in Computer Vision. CVC 2019. Advances in Intelligent Systems and Computing, vol. 944, Springer, Cham, pp. 280–292.
[16] S.A. Kumar, J. Vanualailai, A. Prasad, Distributed velocity controllers of the individuals of emerging swarm clusters, in: 2020 IEEE Asia-Pacific Conference on Computer Science and Data Engineering (CSDE), 2020, pp. 1–6, doi:10.1109/CSDE50874.2020.9411585.
[17] A. Okubo, S. Levin, Diffusion and Ecological Problems: Modern Perspectives, Interdisciplinary Applied Mathematics, Springer, 2001.
[18] L. Edelstein-Keshet, Mathematical models of swarming and social aggregation, in: Procs. 2001 International Symposium on Nonlinear Theory and Its Applications, Miyagi, Japan, 2001, pp. 1–7.
[19] A. Mogilner, L. Edelstein-Keshet, A non-local model for a swarm, J Math Biol 38 (1999) 534–570.
[20] S.A. Levin, Complex adaptive systems: exploring the known, the unknown and the unknowable, Bulletin of the Americal Mathematical Society 40 (1) (2002) 3–19.
[21] A. Mogilner, L. Edelstein-Keshet, L. Bent, A. Spiros, Mutual interactions, potentials, and individual distance in a social aggregation, J Math Biol 47 (2003) 353–389.
[22] V. Gazi, K.M. Passino, Stability analysis of social foraging swarms, IEEE Transactions on Systems, Man and Cybernetics – Part B 34 (1) (2004) 539–557.
[23] A.J. Merrifield, An Investigation Of Mathematical Models For Animal Group Movement, Using Classical And Statistical Approaches, University of Sydney, NSW, Australia, 2006 Ph.D. thesis.
[24] A. Mansour, A. Y-K., Three-dimensional optimal path planning for waypoint guidance of an autonomous underwater vehicle, Rob Auton Syst 67 (2015) 23–32. Advances in Autonomous Underwater Robotics
[25] A. Bais, R. Sablatnig, Landmark based global self-localization of mobile soccer robots, in: Lecture Notes in Computer Science, Hydrabad, India, 2006, pp. 842–851.
[26] A. Dawadee, J. Chahl, N. Nandagopal, A method for autonomous navigation of UAVs using landmarks, in: Proceedings of the 16th Australian Aerospace Congress, 2015.
[27] A. Prasad, B. Sharma, J. Vanualailai, S. Kumar, Stabilizing controllers for landmark navigation of planar robots in an obstacle-ridden workspace, Journal of Advanced Transportation 2020 (2020), doi:10.1155/2020/8865608.
[28] A.J. Briggs, C. Detweiler, D. Scharstein, A. Vandenberg-Rodes, Expected shortest paths for landmark-based robot navigation, Int J Rob Res 23 (7–8) (2004) 717–728, doi:10.1177/0278364904045467.
[29] H. Fujii, Y. Ando, T. Yoshimi, M. Mizukawa, Shape recognition of metallic landmark and its application to self-position estimation for mobile robot, Journal of Robotics and Mechatronics 22 (6) (1999) 718–725.
[30] H. Hu, D. Gu, Landmark-based navigation of mobile robots in manufacturing, in: Proceedings of the IEEE International Conference on Emerging Technologies and factory Automation, 1999, pp. 121–128.
[31] P. Boucher, Waypoints guidance of differential-drive mobile robots with kinematic and precision constraints, Robotica 32 (2014) 1–24, doi:10.1017/S0263574714001921.
[32] E. Keyder, S. Richter, M. Helmert, Sound and complete landmarks for and/or graphs, ECAI, 2010.
[33] K. Erez, D. Carmel, Cost-optimal planning with landmarks, in: Proceedings of the 21st International Jont Conference on Artifical Intelligence, in: IJCAI'09, Morgan Kaufmann Publishers Inc., San Francisco, CA, USA, 2009, pp. 1728–1733.
[34] M. Elkawkagy, B. Schattenberg, S. Biundo-Stephan, Landmarks in hierarchical planning, ECAI, 2010.
[35] L. Frommberger, Representing and Selecting Landmarks in Autonomous Learning of Robot Navigation, vol. 5314, Springer, pp. 488–497.
[36] M. Beinhofer, J. Müller, A. Krause, W. Burgard, Robust landmark selection for mobile robot navigation., in: Proc. of the IEEE Int. Conf. on Intelligent Robots and Systems (IROS), 2013.
[37] F. Ducatelle, G. Di Caro, A. Förster, M. Bonani, M. Dorigo, S. Magnenat, F. Mondada, R. O' Grady, C. Pinciroli, P. Rétornaz, V. Trianni, L.M. Gambardella, Cooperative navigation in robotic swarms, Swarm Intell. 8 (2014) 1–33.
[38] S. Singh, P. Sujit, Landmarks based path planning for UAVs in GPS-denied areas, IFAC-PapersOnLine 49 (1) (2016) 396–400.
[39] R. Ramaithititima, S. Bhattacharya, Landmark-based exploration with swarm of resource constrained robots, in: 2018 IEEE International Conference on Robotics and Automation (ICRA), 2018, pp. 5034–5041.
[40] C.W. Reynolds, Flocks, herds, and schools: A distributed behavioral model, in computer graphics, in: Proceedings of the 14th Annual Conference on Computer Graphics and Interactive Techniques, New York, USA, 1987, pp. 25–34.
[41] D. Liberzon, A.S. Morse, Basic problems in stability and design of switched systems, Control Systems, IEEE 19 (5) (1999) 59–70.
[42] S.A. Kumar, J. Vanualailai, B. Sharma, Lyapunov-based control for a swarm of planar nonholonomic vehicles, Mathematics in Computer Science 9 (4) (2015) 461–475.
[43] V. Gazi, K. Passino, Stability analysis of swarms, IEEE Trans Automat Contr 48 (2003) 692–697.
[44] S.A. Kumar, J. Vanualailai, B. Sharma, A. Prasad, Velocity controllers for a swarm of unmanned aerial vehicles, Journal of Industrial Information Integration 22 (2021) 100198, doi:10.1016/j.jii.2020.100198.
[45] B. Sharma, S. Singh, J. Vanualailai, A. Prasad, Globally rigid formation of n-link doubly nonholonomic mobile manipulators, Rob Auton Syst 2018 (2018) 69–84.
[46] B. Wohlfender, Studies on Mechatronics: Autonomous Collaborative Vehicles, 2010.
[47] G.F.L. D'Alfonso, G. Fedele, Distributed model predictive control for constrained multi-agent systems: a swarm aggregation approach, in: 2018 Annual American Control Conference (ACC), 2018, pp. 5082–5087, doi:10.23919/ACC.2018.8431392.
[48] H.W.D. Hettiarachchi, K.T.M.U. Hemapala, A.G.B.P. Jayasekara, Review of applications of fuzzy logic in multi-agent-based control system of AC-DC hybrid microgrid, IEEE Access 7 (2019) 1284–1299, doi:10.1109/ACCESS.2018.2884503.
[49] C. Solano-Aragón, A. Alanis, Multi-agent system with fuzzy logic control for autonomous mobile robots in known environments, in: O. Castillo, W. Pedrycz, K. J. (Eds.), Evolutionary Design of Intelligent Systems in Modeling, Simulation and Control. Studies in Computational Intelligence, 275, Springer, Berlin, Heidelberg, 2009, pp. 33–52, doi:10.1007/978-3-642-04514-1_3.
[50] M. Sisto, D. Gu, A fuzzy leader-follower approach to formation control of multiple mobile robots, 2006 IEEE/RSJ International Conference on Intelligent Robots and Systems (2006) 2515–2520.
[51] G.G. Rigatos, Distributed gradient and particle swarm optimization for multi-robot motion planning, Robotica 26 (3) (2008) 357–370, doi:10.1017/S0263574707004080.
[52] R. Olfati-Saber, R.M. Murray, Graph rigidity and distributed formation stabilization of multi-vehicle systems, in: Proceedings of the 41st IEEE Conference on Decision and Control, 2002., 3, 2002, pp. 2965–2971 vol.3, doi:10.1109/CDC.2002.1184307.
[53] M. Mesbahi, M. Egerstedt, Graph Theoretic Methods in Multiagent Networks, Princeton University Press, NJ, 2010.
[54] B. Sharma, J. Vanualailai, A. Prasad, A dø-strategy: facilitating dual-formation control of a virtually connected team, Journal of Advanced Transportation 2017 (2017) 1–17.
[55] K. Raghuwaiya, B. Sharma, J. Vanualailai, Leader-follower based locally rigid formation control, Journal of Advanced Transportation 2018 (2018) 1–14.
[56] B. Sharma, J. Vanualailai, A. Prasad, Formation control of a swarm of mobile manipulators, Rocky Mountain Journal of Mathematics 41 (3) (2011) 909–940.
[57] G.J. Pappas, K.J. Kyriakopoulos, Stabilisation of non-holonomic vehicle under kinematic constraints, Int J Control 61 (4) (1995) 933–947.
[58] M.S. Branicky, Multiple Lyapunov fuctions and other analysis tools for switched and hybrid systems, IEEE Trans Automat Contr 43 (4) (1998) 475–482.